Title
Backscattering of Continuous and Pulsed Beams

Journal
Multiscale Modeling and Simulation, 15(4)

ISSN
1540-3459

Authors
Rohde, Shelley B
Kim, Arnold D

Publication Date
2017

DOI
10.1137/16m1072097

Peer reviewed

MULTISCALE MODEL. SIMUL.
Vol. 15, No. 4, pp. 1356–1375

BACKSCATTERING OF CONTINUOUS AND PULSED BEAMS*

SHELLEY B. ROHDE† AND ARNOLD D. KIM‡

Abstract. We study the light backscattered by a half space composed of an absorbing and scattering medium due to a continuous and pulsed collimated beam obliquely incident on the boundary. This problem has several applications, but we focus our attention here on midinfrared diffuse reflectance spectroscopy. For that problem, one seeks to determine the absorption spectrum due to a weakly absorbing analyte mixed with a strongly scattering medium. The theory of radiative transfer is used to model this problem. In particular, we apply a systematic asymptotic analysis on the boundary value problem for the continuous beam and the initial-boundary value problem for the pulsed beam and obtain a simple model for the diffuse reflectance that accurately captures its multiscale behavior in space and time. We validate the results of this asymptotic analysis through comparisons with numerical results computed from the full radiative transfer equation.

Key words. multiple light scattering, radiative transfer, diffusion, diffuse reflectance spectroscopy

AMS subject classifications. 34E15, 35Q60, 78A45, 78A48

DOI. 10.1137/16M1072097

1. Introduction.

We study light backscattering by a half space composed of a multiple scattering medium due to a collimated beam obliquely incident on its boundary. This problem is fundamental for several applications, including biomedical optics [34], geophysical remote sensing [31], and computer graphics [14], to name a few. However, we focus our attention here on the specific problem of midinfrared diffuse reflectance spectroscopy [6, 3, 22].

For the midinfrared diffuse reflectance spectroscopy problem, the objective is to recover the absorption coefficient as a function of wavelength, i.e., the absorption spectrum, of a weakly absorbing analyte over midinfrared wavelengths. Since the midinfrared range of wavelengths corresponds to the fundamental vibrations and associated rotational-vibrational structure of molecules, analytical chemists use this absorption spectrum to identify the chemical compositions of environmental and forensic samples, for example, and their respective concentrations. Sample sizes of an analyte are typically very small. Therefore, one cannot obtain enough net absorption from a direct optical probing to recover the absorption spectrum. Instead, one mixes the sample in a strongly scattering, nonabsorbing medium, e.g., KBr ground to a fine powder. By introducing a strong multiple scattering background medium, one effectively increases the net absorption by the analyte. The key challenge lies in interpreting measurements of light backscattered by these samples.

The theory of radiative transfer [2] is appropriate for modeling this problem. This theory accurately takes into account absorption and scattering by inhomogeneities in the medium. Moreover, when scattering is dominant, we may apply the diffusion approximation to the radiative transfer equation. The diffusion approximation applies to light that has penetrated deep into a strong multiple scattering medium. For that

*Received by the editors April 24, 2016; accepted for publication (in revised form) May 16, 2017; published electronically October 10, 2017.
http://www.siam.org/journals/mms/15-4/M107209.html
†Department of Mathematical and Computer Sciences, Metropolitan State University of Denver, Denver, CO 80217 (srohde2@msudenver.edu).
‡Applied Mathematics Unit, School of Natural Sciences, University of California, Merced, Merced, CA 95343 (adkim@ucmerced.edu).

case, the leading order asymptotic behavior of the intensity is governed by a much simpler diffusion equation. Larsen and Keller [24] introduced a systematic asymptotic analysis of this problem. That work provides the framework to derive boundary data and sources for the diffusion equation.

The diffusion approximation has been used extensively as a simplification of the radiative transfer equation to model multiple scattering of light, especially for biomedical optics applications [11, 34]. In fact, there are several studies in the applied literature where the diffusion approximation is used to model the problem we seek to study here [12, 27, 16]. However, researchers have used various phenomenological models for boundary conditions and sources, e.g., [4, 23, 10, 30, 8, 9, 15, 5, 13, 33], instead of the systematic asymptotic analysis. Among all of these models, the most commonly used model for an infinitesimally narrow, collimated beam incident on the boundary of a multiple scattering medium is to place a single, isotropic point source sufficiently deep in the medium below the boundary surface. For example, Wang and Jacques [32] use a single isotropic point source placed off-axis to model an obliquely incident collimated beam. Using an isotropic point source to model a collimated beam is clearly a very crude approximation to the actual problem, and researchers are aware that these models are prone to substantial errors [33]. Nonetheless, this model has been and is still used extensively in practice because it is easy to use and retains useful qualitative features of the diffuse reflectance for large distances away from the beam center and over long times after the pulse has impinged on the medium.

A recent technological advancement by Brauns [1] has led to ultrafast measurements of the midinfrared diffuse reflectance due to femtosecond pulses. These measurements are generated by difference frequency mixing the output of an optical parametric amplifier that is pumped by a regeneratively amplified Ti:Sapphire laser. Time resolution is achieved by up-converting the diffusely reflected photons with pulses from the Ti:Sapphire oscillator. This instrument, which is capable of studying midinfrared diffuse reflectance with femtosecond time resolution, provides unprecedented access to the effective path lengths that photons travel in a strongly scattering medium. Because the aforementioned crude approximation using an isotropic point source was found to be insufficient to fit the data, a biexponential model for the time dependence of the diffuse reflectance was used a posteriori to interpret these measurements.

It is our objective here to provide a quantitatively accurate and intuitive mathematical model to interpret ultrafast measurements of the diffuse reflectance. The key to this problem is taking into account the inherent multiple scales in space and time. To study this problem, we review the asymptotic analysis for the diffusion approximation. In applying this asymptotic analysis to this problem, we find that the diffuse reflectance requires a higher order asymptotic approximation to capture its leading order asymptotic behavior. We also find that the analysis for a pulsed beam problem is a simple extension of the continuous beam problem. Both problems are useful for many different applications beyond the one discussed here. Consequently, we present results for both of these problems. Our main result is an asymptotic model for the time-dependent, midinfrared diffuse reflectance that captures the features observed by Brauns and describes them in terms of fundamental, optical properties of the medium.

The remainder of this paper is as follows. We give the formulation of the boundary value problem for the continuous beam and the initial-boundary value problem for the pulsed beam in section 2. In section 3, we apply an asymptotic analysis to solve these boundary value and initial-boundary value problems. In section 4, we discuss the method used for computing the boundary layer solution and its asymptotic behavior.

In section 5, we give our asymptotic model for the diffuse reflectance. We validate this asymptotic model through comparisons with full numerical solutions of the radiative transfer equation in section 6. Section 7 is our conclusions.

2. Formulation. The radiative transfer equation,

$$\partial_t I + \hat{\mathbf{s}} \cdot \nabla I + \mu_a I + \mu_s L I = Q, \tag{2.1}$$

governs the intensity $I : S^2 \times \mathbb{R}^3 \times [0,T] \to \mathbb{R}^+ \geq 0$ in a medium that absorbs, scatters, and emits light. Here, we assume that (2.1) has already been nondimensionalized in a physically meaningful way. The nonnegative absorption and scattering coefficients are denoted by μ_a and μ_s, respectively. The scattering operator, L, is defined as

$$LI = I - \int_{S^2} p(\hat{\mathbf{s}} \cdot \hat{\mathbf{s}}') I(\hat{\mathbf{s}}', \mathbf{r}, t) \mathrm{d}\hat{\mathbf{s}}' \tag{2.2}$$

with p denoting the scattering phase function. The scattering phase function gives the fraction light incident in direction $\hat{\mathbf{s}}'$ that is scattered in direction $\hat{\mathbf{s}}$. The nonhomogeneous term, Q, is an interior light source.

Notice that we have assumed that p is spherically symmetric so that it depends only on $\hat{\mathbf{s}} \cdot \hat{\mathbf{s}}'$. Consequently, it can be written as an expansion in Legendre polynomials,

$$p(\hat{\mathbf{s}} \cdot \hat{\mathbf{s}}') = \sum_{l=0}^{\infty} \frac{2l+1}{4\pi} \xi_l P_l(\hat{\mathbf{s}} \cdot \hat{\mathbf{s}}'), \tag{2.3}$$

with $\{P_l\}$ denoting the set of Legendre polynomials, and

$$\xi_l = 2\pi \int_{-1}^{1} p(\hat{\mathbf{s}} \cdot \hat{\mathbf{s}}') P_l(\hat{\mathbf{s}} \cdot \hat{\mathbf{s}}') \mathrm{d}(\hat{\mathbf{s}} \cdot \hat{\mathbf{s}}'). \tag{2.4}$$

Conservation of power requires that $\xi_0 = 1$. Using the addition theorem, we can represent $P_l(\hat{\mathbf{s}} \cdot \hat{\mathbf{s}}')$ as

$$P_l(\hat{\mathbf{s}} \cdot \hat{\mathbf{s}}') = \frac{4\pi}{2l+1} \sum_{m=-l}^{l} Y_{lm}(\hat{\mathbf{s}}) Y_{lm}^*(\hat{\mathbf{s}}'), \quad l \geq 0, \tag{2.5}$$

with $\{Y_{lm}(\hat{\mathbf{s}})\}$ denoting the set of spherical harmonics. Substituting (2.5) into (2.3), we find that

$$p(\hat{\mathbf{s}} \cdot \hat{\mathbf{s}}') = \sum_{l=0}^{\infty} \xi_l \sum_{m=-l}^{l} Y_{lm}(\hat{\mathbf{s}}) Y_{lm}^*(\hat{\mathbf{s}}'). \tag{2.6}$$

Consequently, we find that

$$L Y_{lm}(\hat{\mathbf{s}}) = (1 - \xi_l) Y_{lm}(\hat{\mathbf{s}}), \tag{2.7}$$

so $1 - \xi_l$ is an eigenvalue of L with corresponding eigenfunction $Y_{lm}(\hat{\mathbf{s}})$. We make use of (2.7) throughout section 3.

We seek to study the light backscattered by a medium composed of a homogeneous mixture of a weakly absorbing analyte and a background scattering medium. For diffuse reflectance spectroscopy problems, the sample is sufficiently large compared to the width of the incident beam and the resulting diffuse reflectance that one may model it as a half space. Let $\Omega = \{\mathbf{r} \in \mathbb{R}^3, z > 0\}$ denote this half space with boundary $\partial\Omega = \{z = 0\}$. We now define the boundary value and initial-boundary value problems for the continuous and pulsed beam problems, respectively.

2.1. Continuous beam problem. To study light backscattered by the half space due to a continuous collimated beam obliquely incident on its boundary, we study the following boundary value problem for the time-independent radiative transfer equation:

$$\hat{\mathbf{s}} \cdot \nabla \tilde{I} + \mu_a \tilde{I} + \mu_s L \tilde{I} = 0 \quad \text{in } S^2 \times \Omega, \tag{2.8a}$$

$$\tilde{I} = T^{\text{in}}[\tilde{I}_b] + R[\tilde{I}] \quad \text{on } \tilde{\Gamma}_{\text{in}} = \{(\hat{\mathbf{s}}, \mathbf{r}) \in S^2 \times \partial\Omega, \hat{\mathbf{s}} \cdot \hat{z} > 0\}. \tag{2.8b}$$

We further require that $\tilde{I} \to 0$ as $z \to \infty$. Note that boundary condition (2.8b) is prescribed only on the hemisphere of directions that point into the medium. $\tilde{I}_b$ is the intensity on $\partial\Omega$ from outside of Ω due to an obliquely incident collimated beam. Let θ_i denote the angle of incidence and $\mu_i = \cos\theta_i$. We set the xz-plane to be the plane of incidence so that

$$\tilde{I}_b = \delta(\mu - \mu_i)\delta(\varphi) f_0(\mu_i x, y), \tag{2.9}$$

where θ is the polar angle with $\mu = \cos\theta$, φ is the azimuthal angle, and f_0 gives the spatial distribution of the incident beam intensity on the plane transverse to its propagation direction. In boundary condition (2.8b), $T^{\text{in}}[\tilde{I}_b]$ denotes the transmission of $\tilde{I}_b$ into Ω, and $R[\tilde{I}]$ denotes the internal reflection of light incident on $\partial\Omega$ from within the half space. We specify these quantities below.

The medium inside the half space has a different refractive index than that outside of it. Let θ_0 denote the angle at which the beam is transmitted into the half space given by Snell's law, $\sin\theta_i = n_{\text{rel}} \sin\theta_0$ with $n_{\text{rel}} > 1$ denoting the ratio of the refractive index inside the half space over that outside of it. Furthermore, let $t_F^{\text{in}}(\mu_0, \mu_i)$ denote the Fresnel transmission coefficient for light incident on the boundary from outside of the half space at $\mu_i = \cos\theta_i$ and transmitted into the half space at $\mu_0 = \cos\theta_0$. It is given by

$$t_F^{\text{in}}(\mu_0, \mu_i) = \frac{n_{\text{rel}}^3 \mu_0}{2\mu_i} \left[\left| \frac{2 n_{\text{rel}} \mu_i}{\mu_i + n_{\text{rel}} \mu_0} \right|^2 + \left| \frac{2 n_{\text{rel}} \mu_i}{n_{\text{rel}} \mu_i + \mu_0} \right|^2 \right]. \tag{2.10}$$

It follows that

$$T^{\text{in}}[\tilde{I}_b] = \delta(\mu - \mu_0)\delta(\varphi) t_F^{\text{in}}(\mu_0, \mu_i) f_0(\mu_i x, y), \quad 0 < \mu \le 1. \tag{2.11}$$

Since $n_{\text{rel}} > 1$, there exists a critical angle θ_c defined through the relation $\sin\theta_c = 1/n_{\text{rel}}$. Let $\mu_c = \cos\theta_c$. For angles less than θ_c, the angle of incidence is equal to the angle of reflectance. For angles larger than θ_c, we have total internal reflection. Let $r_F(\mu)$ denote the Fresnel reflection coefficient for light incident on the boundary from within the half space in direction θ where $\mu = \cos\theta$. It is given by

$$r_F(\mu) = \begin{cases} 1, & 0 < \mu \le \mu_c, \\ \dfrac{1}{2} \left| \dfrac{n_{\text{rel}} \Upsilon(\mu) - \mu}{n_{\text{rel}} \Upsilon(\mu) + \mu} \right|^2 + \dfrac{1}{2} \left| \dfrac{n_{\text{rel}} \mu - \Upsilon(\mu)}{n_{\text{rel}} \mu + \Upsilon(\mu)} \right|^2, & \mu_c < \mu \le 1, \end{cases} \tag{2.12}$$

with $\Upsilon(\mu) = \sqrt{1 - n_{\text{rel}}^2 (1 - \mu^2)}$ corresponding to the direction of light from within Ω transmitted across $\partial\Omega$ given by Snell's law. It follows that

$$R[\tilde{I}] = r_F(\mu) \tilde{I}(-\mu, \varphi, x, y, 0), \quad 0 < \mu \le 1. \tag{2.13}$$

The steady-state diffuse reflectance, $\tilde{R}_d$, measures the spatial distribution of power backscattered by the medium. It is defined in terms of $\tilde{I}$ satisfying boundary value problem (2.8) as

$$\tilde{R}_d(x,y) = \int_{\hat{\mathbf{s}}\cdot\hat{z}<0} T^{\text{out}}[\tilde{I}](\hat{\mathbf{s}}, x', y', 0)\hat{\mathbf{s}}\cdot(-\hat{z})\mathrm{d}\hat{\mathbf{s}}. \tag{2.14}$$

Here, T^{out} denotes the operator that maps the light incident on $\partial\Omega$ from within Ω to that transmitted outside of Ω. Let $t_F^{\text{out}}(\mu) = 1 - r_F(-\Upsilon^{-1}(\mu))$ with $\Upsilon^{-1}(\mu) = \sqrt{1-(1-\mu^2)/n_{\text{rel}}^2}$. Then,

$$T^{\text{out}}[\tilde{I}] = t_F^{\text{out}}(\mu)\tilde{I}(\Upsilon^{-1}(\mu), \varphi, x, y, 0), \quad -1 \le \mu < 0, \tag{2.15}$$

and so

$$\tilde{R}_d(x,y) = -\int_0^{2\pi}\int_{-1}^{0} t_F^{\text{out}}(\mu)\tilde{I}(\Upsilon^{-1}(\mu), \varphi, x, y, 0)\mu\mathrm{d}\mu\mathrm{d}\varphi. \tag{2.16}$$

2.2. Pulsed beam problem. To study light backscattered by a multiple scattering medium due to a pulsed collimated beam obliquely incident on its boundary, we study the following initial-boundary value problem for the time-dependent radiative transfer equation:

$$\partial_t I + \hat{\mathbf{s}}\cdot\nabla I + \mu_a I + \mu_s L I = 0 \quad \text{in } S^2\times\Omega\times(0,T], \tag{2.17a}$$

$$I = T^{\text{in}}[I_b] + R[I] \quad \text{on } \Gamma_{\text{in}} = \{(\hat{\mathbf{s}}, \mathbf{r}, t) \in S^2\times\partial\Omega\times(0,T], \hat{\mathbf{s}}\cdot\hat{z} > 0\}, \tag{2.17b}$$

$$I(\hat{\mathbf{s}}, \mathbf{r}, 0) = 0 \quad \text{on } S^2\times\Omega. \tag{2.17c}$$

We also require that $I \to 0$ as $z \to \infty$ for this initial-boundary value problem. Here, boundary condition (2.17b) is extended to include a time-dependent source so that for this problem,

$$T^{\text{in}}[I_b] = \delta(\mu-\mu_0)\delta(\varphi)t_F^{\text{in}}(\mu_0,\mu_i)f(\mu_i x, y, t), \quad 0 < \mu \le 1. \tag{2.18}$$

For convenience, let $F(x,y,t) = t_F^{\text{in}}(\mu_0,\mu_i)f(\mu_i x, y, t)$. Because the only source of light in this problem is the beam incident on the boundary, initial condition (2.17c) prescribes no light in the system at $t = 0$.

The time-dependent diffuse reflectance, R_d, measures the spatial-temporal distribution of power backscattered by the medium. It is given in terms of the solution of initial-boundary value problem (2.17) as

$$R_d(x,y,t) = \int_{\hat{\mathbf{s}}\cdot\hat{z}<0} T^{\text{out}}[I](\hat{\mathbf{s}}, x, y, 0, t)\hat{\mathbf{s}}\cdot(-\hat{z})\mathrm{d}\hat{\mathbf{s}}. \tag{2.19}$$

3. Asymptotic analysis. We may obtain the solution of boundary value problem (2.8) as a special case of initial-boundary value problem (2.17). Therefore, we focus our discussion here on the asymptotic solution of initial-boundary value problem (2.17). After solving that problem, we specialize that result to obtain the solution of boundary value problem (2.8).

We seek the asymptotic solution of (2.17) when scattering is strong and absorption is weak. To make this assumption explicit, we introduce the small parameter, $0 < \epsilon \ll 1$, and set $\mu_s = 1/\epsilon$ and $\mu_a = \epsilon\alpha$ leading to the rescaled equation

$$\epsilon^2\partial_t I + \epsilon\hat{\mathbf{s}}\cdot\nabla I + \epsilon^2\alpha I + LI = 0. \tag{3.1}$$

We have introduced $\alpha = O(1)$ to explicitly allow us to keep track of how the diffuse reflectance depends on the absorption coefficient. Equation (3.1) is to be solved in $S^2 \times \Omega \times (0, T]$ subject to boundary condition (2.17b) and initial condition (2.17c). It is a singularly perturbed problem. In the most general setting, we would need to consider the interior solution, the boundary layer solution, the initial layer solution, and the boundary-initial layer solution [24]. However, since initial condition (2.17c) prescribes that $I = 0$ everywhere in the domain, no initial layer solution is needed. Moreover, assuming that the pulsed beam does not inject any light into the medium before $t = 0^+$, we remove the need for an initial-boundary layer solution. Therefore, the asymptotic solution is given as the sum

$$I = \Phi + \Psi, \tag{3.2}$$

where Φ denotes the interior solution and Ψ denotes the boundary layer solution. We now compute asymptotic expansions for Φ and Ψ in the limit as $\epsilon \to 0$. We show below that we need an asymptotic approximation accurate to $O(\epsilon^2)$ to capture the key features of the diffuse reflectance.

3.1. Interior solution. We seek an asymptotic solution of Φ as the following power series in ϵ:

$$\Phi \sim \sum_{n=0}^{\infty} \epsilon^n \phi_n, \quad \epsilon \to 0. \tag{3.3}$$

Substituting (3.3) into (3.1) and collecting like powers of ϵ, we obtain

$$L\phi_0 = 0, \tag{3.4a}$$

$$L\phi_1 = -\hat{\mathbf{s}} \cdot \nabla \phi_0, \tag{3.4b}$$

$$L\phi_n = -\hat{\mathbf{s}} \cdot \nabla \phi_{n-1} - \partial_t \phi_{n-2} - \alpha \phi_{n-2}, \quad n \geq 2. \tag{3.4c}$$

The spectrum of L is given in (2.7) with $\xi_0 = 1$. From (2.7), we find that any function proportional to $Y_{00}(\hat{\mathbf{s}})$ lies in the kernel of L. From this we conclude that ϕ_0 satisfying (3.4a) must be an isotropic function, which we denote by $\phi_0 = \rho_0(\mathbf{r}, t)$. It can be shown through direct substitution that $\hat{\mathbf{s}} \cdot \nabla \rho_0$ is an eigenfunction of L with eigenvalue $1 - \xi_1$. Consequently, we find that $\phi_1 = \rho_1 - \hat{\mathbf{s}} \cdot \nabla \rho_0 / (1 - \xi_1)$ with $\rho_1(\mathbf{r}, t)$ denoting another isotropic function. Substituting these results into (3.4c) evaluated at $n = 2$, we obtain

$$L\phi_2 = -\hat{\mathbf{s}} \cdot \nabla \rho_1 + \hat{\mathbf{s}} \cdot \nabla \left(\frac{\hat{\mathbf{s}} \cdot \nabla \rho_0}{1 - \xi_1} \right) - \partial_t \rho_0 - \alpha \rho_0. \tag{3.5}$$

For (3.5) to be solvable, its right-hand side must be orthogonal to $Y_{00}(\hat{\mathbf{s}})$. Integrating the right-hand side of (3.5) with respect to $\hat{\mathbf{s}}$ over the unit sphere, and setting that result to zero, we obtain the diffusion equation,

$$\partial_t \rho_0 - \kappa \mathit{\Delta} \rho_0 + \alpha \rho_0 = 0, \tag{3.6}$$

with $\kappa = [3(1 - \xi_1)]^{-1}$ denoting the diffusion coefficient, and $\mathit{\Delta}$ denoting the laplacian. With ρ_0 satisfying (3.6), we find that ϕ_2 is given by

$$\phi_2 = \rho_2 - \frac{\hat{\mathbf{s}} \cdot \nabla \rho_1}{1 - \xi_1} + \sum_{m=-2}^{2} \frac{Y_{2,m}(\hat{\mathbf{s}}) A_m \rho_0}{1 - \xi_2}, \tag{3.7}$$

with $\rho_2(\mathbf{r},t)$ denoting an isotropic function, and the operators, A_m for $m=-2,\dots,2$, are defined as

$$A_{-2} = 2\sqrt{\frac{\pi}{30}}(\partial_x^2 - \partial_y^2 + \mathrm{i}\partial_x\partial_y), \tag{3.8}$$

$$A_{-1} = \sqrt{\frac{2\pi}{15}}(\partial_x\partial_z + \mathrm{i}\partial_y\partial_z), \tag{3.9}$$

$$A_0 = \frac{2}{3}\sqrt{\frac{\pi}{5}}(-\partial_x^2 - \partial_y^2 + 2\partial_z^2), \tag{3.10}$$

$$A_1 = \sqrt{\frac{2\pi}{15}}(-\partial_x\partial_z + \mathrm{i}\partial_y\partial_z), \tag{3.11}$$

$$A_2 = 2\sqrt{\frac{\pi}{30}}(\partial_x^2 - \partial_y^2 - \mathrm{i}\partial_x\partial_y). \tag{3.12}$$

Substituting (3.7) into (3.4c) evaluated at $n=3$, we obtain

$$L\phi_3 = -\hat{\mathbf{s}}\cdot\nabla\rho_2 + \hat{\mathbf{s}}\cdot\nabla\left(\frac{\hat{\mathbf{s}}\cdot\nabla\rho_1}{1-\xi_1}\right) - \sum_{m=-2}^{2}\frac{\hat{\mathbf{s}}\cdot\nabla\left[Y_{2,m}(\hat{\mathbf{s}})A_m\rho_0\right]}{1-\xi_2} - \partial_t\rho_1 - \alpha\rho_1. \tag{3.13}$$

By integrating the right-hand side of (3.13) with respect to $\hat{\mathbf{s}}$ over the unit sphere, we find that ρ_1 satisfies the same diffusion equation as ρ_0 in (3.6). We can continue on with this procedure to determine higher order terms.

At this point, we have found that the interior solution is given by

$$\Phi = \rho_0 + \epsilon\left[\rho_1 - \hat{\mathbf{s}}\cdot(3\kappa\nabla\rho_0)\right] + O(\epsilon^2), \tag{3.14}$$

with ρ_0 and ρ_1 both satisfying the diffusion equation given in (3.6). These diffusion equations are to be solved in the half space, Ω, subject to initial conditions

$$\rho_0(\mathbf{r},0) = \rho_1(\mathbf{r},0) = 0. \tag{3.15}$$

Additionally, we require that $\rho_0, \rho_1 \to 0$ as $z\to\infty$. We are missing boundary conditions for ρ_0 and ρ_1 on $\partial\Omega$. To obtain these boundary conditions, we must compute the boundary layer solution, which we discuss below.

Several previous works on this topic [18, 21, 25, 29] did not include the isotropic function, ρ_1, in the computation of the interior solution, which was an oversight. In fact, this isotropic function is needed here to compute a formally correct asymptotic approximation to $O(\epsilon^2)$. Although the inclusion of this additional term is mentioned by Larsen and Keller [24] and Habetler and Matkowsky [7], other works [26, 28] only indicate that the diffusion equation is accurate to $O(\epsilon^2)$ but do not include a term like ρ_1 to justify it. Omitting this term leads to a formal error in the asymptotic expansion. However, this formal error does not adversely affect the final results contained in the aforementioned previous works because both ρ_0 and ρ_1 satisfy the same diffusion equation. We explain this matter in detail at the end of section 4.

3.2. Boundary layer solution. We cannot obtain an appropriate boundary condition for the interior solution just by substituting (3.14) into (2.17b), which is why we include the boundary layer solution, Ψ. Substituting (3.14) into (3.2) and then substituting that result with (2.18) into (2.17b), we obtain

$$\begin{aligned}\Psi - R[\Psi] = {} & \delta(\mu-\mu_0)\delta(\varphi)F - \rho_0 - \epsilon\rho_1 + \epsilon\hat{\mathbf{s}}\cdot(3\kappa\nabla\rho_0)\\ & + R\left[\rho_0 + \epsilon\rho_1 - \epsilon\hat{\mathbf{s}}\cdot(3\kappa\nabla\rho_0)\right] + O(\epsilon^2) \quad \text{on } \Gamma_{\text{in}}.\end{aligned} \tag{3.16}$$

Boundary condition (3.16) shows that Ψ will correct errors made by Φ at the boundary.

Next, we require that Ψ satisfies (3.1). To focus our attention on and near the boundary, $z = 0$, we introduce the stretched variable, $z = \epsilon\zeta$, and let $\psi(\hat{\mathbf{s}}, x, y, \zeta) = \Psi(\hat{\mathbf{s}}, x, y, \epsilon\zeta)$. By making these changes of variables in (3.1), we obtain

$$\mu\partial_\zeta\psi + L\psi = -\epsilon\hat{\mathbf{s}}_\perp \cdot \nabla_\perp\psi + O(\epsilon^2). \tag{3.17}$$

Here, $\mu = \hat{\mathbf{s}} \cdot \hat{z}$, $\hat{\mathbf{s}}_\perp = (\hat{\mathbf{s}} \cdot \hat{x}, \hat{\mathbf{s}} \cdot \hat{y})$, and $\nabla_\perp = (\partial_x, \partial_y)$. Equation (3.17) is to be solved in the half space $\zeta > 0$ subject to boundary condition (3.16). We also require that ψ satisfies the following asymptotic matching condition:

$$\psi \to 0 \quad \text{as } \zeta \to \infty. \tag{3.18}$$

Equation (3.18) ensures that the boundary layer solution vanishes outside of the boundary layer whose thickness is $O(\epsilon)$.

There are several important remarks to make at this point. Derivatives in x, y, and t do not appear in (3.17) to leading order. In fact, these variables are just parameters for the boundary layer solution to $O(\epsilon^2)$. Consequently, we are to solve a much simpler one- (spatial-) dimensional problem. With regards to the parametric dependence on t, this result will have an important implication for the short time behavior of the asymptotic solution. In addition, there is no absorption. As a result, $\psi =$ constant solves (3.17) to $O(\epsilon^2)$. In fact, the constant solution is the only one that does not satisfy asymptotic matching condition (3.18). Thus, by determining how boundary condition (3.16) and the nonhomogeneous terms in (3.17) map to the constant solution, we will find conditions on F, ρ_0, and ρ_1 that will lead to the desired boundary conditions for ρ_0 and ρ_1. In the following section, we describe a method to solve this boundary layer problem and obtain the results needed to compute the boundary condition sought for the diffusion equation.

4. Computing the boundary layer solution. To be able to use the asymptotic analysis above to compute the diffuse reflectance, we need to determine the solution of (3.17), which we write as $\psi = \psi_0 + \epsilon\psi_1 + O(\epsilon^2)$. Substituting this asymptotic expansion into (3.16) and (3.17) and collecting like powers of ϵ, we find ψ_0 satisfies the homogeneous problem

$$\mu\partial_\zeta\psi_0 + L\psi_0 = 0 \tag{4.1}$$

in $\zeta > 0$ subject to boundary condition

$$\psi_0 - R[\psi_0] = \delta(\mu - \mu_0)\delta(\varphi)F - \rho_0 + R[\rho_0] \quad \text{on } z = 0 \text{ and } 0 < \mu \leq 1 \tag{4.2}$$

and asymptotic matching condition (3.18). To $O(\epsilon)$, we find that ψ_1 satisfies

$$\mu\partial_\zeta\psi_1 + L\psi_1 = -\hat{\mathbf{s}}_\perp \cdot \nabla_\perp\psi_0 \tag{4.3}$$

in $\zeta > 0$ subject to boundary condition

$$\psi_1 - R[\psi_1] = -\rho_1 + \hat{\mathbf{s}} \cdot (3\kappa\nabla\rho_0) + R[\rho_1 - \hat{\mathbf{s}} \cdot (3\kappa\nabla\rho_0)] \quad \text{on } z = 0 \text{ and } 0 < \mu \leq 1 \tag{4.4}$$

with asymptotic matching condition (3.18).

Because the scattering phase function depends only on $\hat{\mathbf{s}} \cdot \hat{\mathbf{s}}'$, it follows that $p = p(\mu, \mu', \varphi - \varphi')$. Moreover, since p is 2π-periodic in $\varphi - \varphi'$, we write

$$p(\mu, \mu', \varphi - \varphi') = \sum_{k=-\infty}^{\infty} p^{(k)}(\mu, \mu')e^{-\mathrm{i}k(\varphi-\varphi')}, \tag{4.5}$$

where

$$p^{(k)}(\mu,\mu') = \frac{1}{2\pi}\int_0^{2\pi} p(\mu,\mu',\varphi-\varphi')e^{\mathrm{i}k(\varphi-\varphi')}\mathrm{d}(\varphi-\varphi'). \tag{4.6}$$

In light of (4.6), we seek ψ_0 and ψ_1 as Fourier series:

$$\psi_n(\mu,\varphi,x,y,z) = \sum_{k=-\infty}^{\infty} \psi_n^{(k)}(\mu,x,y,z)e^{-\mathrm{i}k\varphi}, \quad n=0,1, \tag{4.7}$$

with $\psi_n^{(k)}$ defined analogously to $p^{(k)}$ in (4.6). Note that because p, ψ_0, and ψ_1 are real functions, $p^{(-k)} = p^{(k)*}$, $\psi_0^{(-k)} = \psi_0^{(k)*}$, and $\psi_1^{(-k)} = \psi_1^{(k)*}$ with a superscript $*$ denoting the complex conjugate. Consequently, it is sufficient to compute these Fourier series coefficients for $k \geq 0$.

Substituting (4.5) and (4.7) into (4.1) and boundary condition (4.2), we find that $\psi_0^{(k)}$ satisfies

$$\mu\psi_{0\zeta}^{(k)} + L_k\psi_0^{(k)} = 0 \tag{4.8}$$

subject to

$$\psi_0^{(k)} - R[\psi_0^{(k)}] = \frac{1}{2\pi}\delta(\mu-\mu_0)F - \delta_{k,0}(1-r_F)\rho_0 \quad \text{on } z=0 \text{ and } 0<\mu\leq 1, \tag{4.9}$$

where $\delta_{k,l}$ denotes the Kronecker delta. Here, L_k is defined as

$$L_k\psi = \psi - \int_{-1}^{1} p^{(k)}(\mu,\mu')\psi(\mu')\mathrm{d}\mu'. \tag{4.10}$$

Similarly, $\psi_1^{(k)}$ satisfies

$$\begin{aligned}\mu\psi_{1\zeta}^{(k)} &+ L_k\psi_1^{(k)} \\ &= -\frac{1}{2}\sqrt{1-\mu^2}\left(\partial_x\psi_0^{(k-1)} - \mathrm{i}\partial_y\psi_0^{(k-1)} + \partial_x\psi_0^{(k+1)} + \mathrm{i}\partial_y\psi_0^{(k+1)}\right)\end{aligned} \tag{4.11}$$

subject to

$$\begin{aligned}\psi_1^{(k)} - R[\psi_1^{(k)}] &= \delta_{k,0}\left[-(1-r_F)\rho_1 + 3\kappa(1+r_F)\mu\partial_z\rho_0\right] \\ &\quad + \frac{3\kappa}{2}(1-r_F)\sqrt{1-\mu^2}\left[\delta_{k,-1}\left(\partial_x\rho_0 - \mathrm{i}\partial_y\rho_0\right) + \delta_{k,1}\left(\partial_x\rho_0 + \mathrm{i}\partial_y\rho_0\right)\right] \\ &\qquad \text{on } z=0 \text{ and } 0<\mu\leq 1.\end{aligned} \tag{4.12}$$

We now solve boundary value problems (4.8) subject to (4.9) and (4.11) subject to (4.12) for the Fourier series coefficients, $\psi_0^{(k)}$ and $\psi_1^{(k)}$, respectively. In particular, we use the fundamental solution for the half space problem to compute these solutions.

4.1. Fundamental solution for the half space problem. Consider the boundary value problem comprising

$$\mu\psi_\zeta + L_k\psi = Q(\mu,\zeta) \quad \text{in } \zeta > 0, \tag{4.13}$$

subject to

$$\psi(\mu,0) - r_F(\mu)\psi(-\mu,0) = B(\mu) \quad \text{on } 0 < \mu \leq 1. \tag{4.14}$$

Note that boundary value problems (4.8) subject to (4.9) and (4.11) subject to (4.12) both take this form. The solution of (4.13) subject to (4.14) is given in terms of the fundamental solution for the half space, $H^{(k)}$, as

$$\begin{aligned}\psi(\mu,\zeta) = &\int_0^\infty \int_{-1}^1 H^{(k)}(\mu,\zeta;\mu',\zeta')Q(\mu',\zeta')\mathrm{d}\mu'\mathrm{d}\zeta' \\ &+ \int_0^1 H^{(k)}(\mu,\zeta;\mu',0)B(\mu')\mu'\mathrm{d}\mu.\end{aligned} \tag{4.15}$$

The fundamental solution for the half space problem satisfies

$$\mu H_\zeta^{(k)} + L_k H^{(k)} = \delta(\mu-\mu')\delta(\zeta-\zeta') \quad \text{in } \zeta,\zeta' > 0 \tag{4.16}$$

subject to

$$H^{(k)}(\mu,0;\mu',\zeta') = r_F(\mu)H^{(k)}(-\mu,0;\mu',\zeta') \quad \text{on } 0 < \mu \leq 1. \tag{4.17}$$

In addition, we require that $H^{(k)}$ is bounded for all $\zeta \neq \zeta'$. We have developed a method to compute $H^{(k)}$ as an expansion in plane wave solutions. Because this method is explained in detail elsewhere [17], we give only the results of this computation below.

Plane wave solutions are special solutions of the form $\psi = e^{\lambda z}V(\mu)$ for the constant coefficient, homogeneous problem

$$\mu\psi_\zeta + \bar{\alpha}\psi + \bar{\sigma}L_k\psi = 0. \tag{4.18}$$

In this, $\bar{\alpha}$ and $\bar{\sigma}$ represent the absorption and scattering coefficients for the general problem. Substituting this ansatz into (4.18), we obtain the generalized eigenvalue problem:

$$\lambda\mu V + \bar{\alpha}V + \bar{\sigma}L_kV = 0. \tag{4.19}$$

We cannot solve (4.19) analytically, in general. Thus, we solve (4.19) numerically. For example, one may use the discrete ordinate method to solve (4.19).

We mention two properties of plane wave solutions that we need here. If the pair $[\lambda, V(\mu)]$ satisfies (4.19), the pair $[-\lambda, V(-\mu)]$ also satisfies (4.19). We also know that two pairs $[\lambda, V(\mu)]$ and $[\lambda', V'(\mu)]$ each satisfying (4.19) satisfy also the orthogonality relation

$$(\lambda - \lambda')\int_{-1}^1 V(\mu)V'(\mu)\mu\mathrm{d}\mu = 0. \tag{4.20}$$

In light of these properties, we order and index the eigenvalues so that

$$\cdots < \mathrm{Re}[\lambda_{-p}] < \cdots < \mathrm{Re}[\lambda_{-1}] < \mathrm{Re}[\lambda_1] < \cdots < \mathrm{Re}[\lambda_p] < \cdots. \tag{4.21}$$

Hence, the symmetry of the plane wave solutions is given by

$$\lambda_{-p} = -\lambda_p, \quad V_{-p}(\mu) = V_p(-\mu), \quad p = 1,2,\ldots. \tag{4.22}$$

We normalize the eigenfunctions according to

$$\int_{-1}^{1} V_p^2(\mu)\mu \mathrm{d}\mu = -\mathrm{sgn}(p). \tag{4.23}$$

In terms of these plane wave solutions, $H^{(k)}$ is given by

$$H^{(k)}(\mu,\zeta;\mu',\zeta') = G^{(k)}(\mu,\zeta;\mu',\zeta') - \sum_{p>0} W_p(\mu) e^{-\lambda_p \zeta} \sum_{q>0} C_{pq} V_q(\mu') e^{-\lambda_q \zeta'} \tag{4.24}$$

with $W_p(\mu) = V_{-p}(\mu) = V_p(-\mu)$ and

$$G^{(k)}(\mu,\zeta;\mu',\zeta') = \begin{cases} \displaystyle\sum_{p>0} V_p(\mu) e^{\lambda_p(\zeta-\zeta')} V_p(\mu'), & \zeta < \zeta', \\ \displaystyle\sum_{p>0} W_p(\mu) e^{-\lambda_p(\zeta-\zeta')} W_p(\mu'), & \zeta > \zeta'. \end{cases} \tag{4.25}$$

The coefficients C_{pq} in (4.24) satisfy the linear system

$$\sum_{p>0} \left[W_p(\mu) - r(\mu) V_p(\mu)\right] C_{pq} = \left[V_q(\mu) - r(\mu) W_q(\mu)\right] \quad \text{on } 0 < \mu \leq 1 \tag{4.26}$$

for $q > 0$.

Now that $H^{(k)}$ is determined explicitly, we substitute it into (4.15) with $Q = 0$ and B given by the right-hand side of (4.9) and find that for $k = 0$,

$$\begin{aligned} \psi_0^{(0)} = {} & \frac{1}{2\pi} H^{(0)}(\mu,\zeta;\mu_0,0)\mu_0 F \\ & - \rho_0(x,y,0,t) \int_0^1 H^{(0)}(\mu,\zeta;\mu',0)[1 - r_F(\mu')]\mu' \mathrm{d}\mu', \end{aligned} \tag{4.27}$$

and for $k > 0$,

$$\psi_0^{(k)} = \frac{1}{2\pi} H^{(k)}(\mu,\zeta;\mu_0,0)\mu_0 F. \tag{4.28}$$

Similarly, we find that $\psi_1^{(0)}$ is given by

$$\begin{aligned} \psi_1^{(0)} = {} & -\int_0^{\infty} \int_{-1}^{1} H^{(0)}(\mu,\zeta;\mu',\zeta') \sqrt{1-\mu'^2} \left(\mathrm{Re}[\partial_x \psi_0^{(1)}] - \mathrm{Im}[\partial_y \psi_0^{(1)}]\right) \mathrm{d}\mu' \mathrm{d}\zeta' \\ & - \rho_1(x,y,0,t) \int_0^1 H^{(0)}(\mu,\zeta;\mu',0)[1 - r_F(\mu')]\mu' \mathrm{d}\mu' \\ & + 3\kappa \partial_z \rho_0(x,y,0,t) \int_0^1 H^{(0)}(\mu,\zeta;\mu',0)[1 + r_F(\mu')]\mu'^2 \mathrm{d}\mu', \end{aligned} \tag{4.29}$$

$\psi_1^{(1)}$ is given by

$$\begin{aligned} \psi_1^{(1)} = {} & -\frac{1}{2} \int_0^{\infty} \int_{-1}^{1} H^{(1)}(\mu,\zeta;\mu',\zeta') \sqrt{1-\mu'^2} \\ & \times \left(\partial_x \psi_0^{(0)} - \mathrm{i}\partial_y \psi_0^{(0)} + \partial_x \psi_0^{(2)} + \mathrm{i}\partial_y \psi_0^{(2)}\right) \mathrm{d}\mu' \mathrm{d}\zeta' \\ & + \frac{3\kappa}{2} \left[\partial_x \rho_0(x,y,0,t) + \mathrm{i}\partial_y \rho_0(x,y,0,t)\right] \int_0^1 H^{(1)}(\mu,\zeta;\mu',0)[1 - r_F(\mu')]\mu'^2 \mathrm{d}\mu', \end{aligned} \tag{4.30}$$

and $\psi_1^{(k)}$ for $k > 1$ is given by

$$\psi_1^{(k)} = -\frac{1}{2}\int_0^\infty \int_{-1}^1 H^{(k)}(\mu,\zeta;\mu',\zeta')\sqrt{1-\mu'^2} \times \left(\partial_x\psi_0^{(k-1)} - \mathrm{i}\partial_y\psi_0^{(k-1)} + \partial_x\psi_0^{(k+1)} + \mathrm{i}\partial_y\psi_0^{(k+1)}\right)\mathrm{d}\mu'\mathrm{d}\zeta'. \tag{4.31}$$

Upon computation of $\psi_0^{(k)}$ and $\psi_1^{(k)}$ for all values of k, we compute ψ_0 and ψ_1 through evaluation of (4.7). The boundary layer solution to $O(\epsilon^2)$ is then given by $\psi = \psi_0 + \epsilon\psi_1 + O(\epsilon^2)$.

4.2. Asymptotic matching. Because the eigenvalues are ordered according to (4.21), we find after substituting (4.24) into (4.15) that the leading order asymptotic behavior of ψ as $z \to \infty$ is given by

$$\psi \sim W_1(\mu)e^{-\lambda_1\zeta}(\beta_V^{(k)} + \beta_S^{(k)}), \quad z \to \infty, \tag{4.32}$$

where

$$\beta_V^{(k)} = \int_0^\infty \int_{-1}^1 e^{\lambda_1\zeta'} W_1(\mu')Q(\mu',\zeta')\mathrm{d}\mu'\mathrm{d}\zeta' - \sum_{q>0} y_{1,q}\int_0^\infty \int_{-1}^1 V_q(\mu')e^{-\lambda_q\zeta'}Q(\mu',\zeta')\mathrm{d}\mu'\mathrm{d}\zeta' \tag{4.33}$$

gives contributions to this leading order asymptotic behavior due to volume sources, and

$$\beta_S^{(k)} = \int_0^1 \left[W_1(\mu') - \sum_{q>0} y_{1,q}V_q(\mu')\right] B(\mu')\mu'\mathrm{d}\mu' \tag{4.34}$$

gives contributions to this leading order asymptotic behavior due to surface sources.

For the special case in which $\bar\alpha \equiv 0$ in (4.19) with $k = 0$, we find that $\lambda = 0$ is an eigenvalue with eigenfunction $V =$ constant. This result is a consequence of $\xi_0 = 1$ in (2.7). Thus, in the limit as $\bar\alpha \to 0^+$, we determine that $\lambda_1 \to 0^+$ and $V_1 \to \bar V_1 =$ constant. Consequently, $\lambda_{-1} \to 0^-$ and $W_1 \to \bar V_1$. The leading order asymptotic behavior given by (4.28) for $k = 0$ gives the only portion of the solution that does not decay exponentially fast as $\zeta \to \infty$. Asymptotic matching condition (3.18) requires setting this leading order asymptotic behavior to zero identically. For this reason, we introduce the functionals

$$\mathscr{P}_V[Q] = \beta_V^{(0)}, \quad \mathscr{P}_S[B] = \beta_S^{(0)}, \quad \bar\alpha \to 0^+. \tag{4.35}$$

In practice, we compute these functionals through evaluation of (4.33) and (4.34) with $k = 0$ and $\bar\alpha \ll 1$ to regularize the numerical solution of (4.19). For example, we set $\bar\alpha = 10^{-8}$ for the calculations shown in section 6.

To derive a boundary condition for the diffusion equation, we examine the requirement of asymptotic matching condition (3.18). To satisfy (3.18), we must prevent a nonzero constant boundary layer solution. With regard to the Fourier series solutions given above, any nonzero constant solution is only due to $\psi_0^{(0)}$ and $\psi_1^{(0)}$.

Because $\psi_0^{(0)}$ satisfies the homogeneous problem given in (4.8) with nonhomogeneous boundary condition (4.9), both evaluated at $k = 0$, we require

$$\mathscr{P}_S\left[\frac{1}{2\pi}\delta(\mu-\mu_0)F - (1-r_F)\rho_0\right] = 0. \tag{4.36}$$

Let

$$a = \mathscr{P}_S[1 - r_F] \tag{4.37}$$

and

$$c = \mathscr{P}_S\left[\frac{1}{2\pi}\delta(\mu - \mu_0)\right]. \tag{4.38}$$

Thus, to satisfy asymptotic matching condition (3.18) to leading order, ρ_0 must satisfy

$$a\rho_0(x, y, 0, t) = cF(x, y, t). \tag{4.39}$$

This Dirichlet boundary condition prescribes the time dependence of ρ_0 evaluated on $z = 0$ to be proportional to the pulsed beam incident on the half space. Consequently, this boundary data gives only the short time behavior of the light backscattered by the half space due to the interior solution.

Because $\psi_1^{(0)}$ satisfies the nonhomogeneous problem given in (4.11) with nonhomogeneous boundary condition (4.12), both evaluated at $k = 0$, we require that

$$\begin{aligned} &\mathscr{P}_V\left[-\sqrt{1-\mu^2}\left(\mathrm{Re}[\partial_x\psi_0^{(1)}] - \mathrm{Im}[\partial_y\psi_0^{(1)}]\right)\right] \\ &\quad - \mathscr{P}_S\left[\rho_1(1 - r_F) - 3\kappa\partial_z\rho_0(1 + r_F)\mu\right] = 0. \end{aligned} \tag{4.40}$$

Substituting (4.28) with $k = 1$ into (4.40), we find that ρ_1 must satisfy

$$a\rho_1(x, y, 0, t) = 3b\kappa\partial_z\rho_0(x, y, 0, t) - \mathbf{d}\cdot\nabla_\perp F(x, y, 0, t). \tag{4.41}$$

Here, a is defined in (4.37),

$$b = \mathscr{P}_S[(1 + r_F)\mu], \tag{4.42}$$

and $\mathbf{d} = (d_1, d_2)$, where

$$d_1 = \frac{\mu_0}{2\pi}\mathscr{P}_V\left[\sqrt{1-\mu^2}\,\mathrm{Re}\left[H^{(1)}(\mu, \zeta, \mu_0, 0)\right]\right] \tag{4.43}$$

and

$$d_2 = -\frac{\mu_0}{2\pi}\mathscr{P}_V\left[\sqrt{1-\mu^2}\,\mathrm{Im}\left[H^{(1)}(\mu, \zeta, \mu_0, 0)\right]\right], \tag{4.44}$$

Boundary condition (4.41) prescribes Dirichlet data for ρ_1. The term proportional to $\partial_z\rho_0$ gives the long time behavior of the light backscattered by the half space. The term proportional to $\nabla_\perp F$ gives a more accurate description of the obliquely incident beam.

Because ρ_0 and ρ_1 satisfy the same diffusion equation, we can consider instead $\rho = \rho_0 + \epsilon\rho_1$, where ρ satisfies the following initial-boundary value problem for the diffusion equation:

$$\partial_t\rho - \kappa\Delta\rho + \alpha\rho = 0 \quad \text{in } \Omega\times(0, T], \tag{4.45a}$$

$$a\rho + \epsilon 3b\kappa\partial_\nu\rho = cF - \epsilon\mathbf{d}\cdot\nabla_\perp F \quad \text{on } \partial\Omega\times(0, T], \tag{4.45b}$$

$$\rho(x, y, z, 0) = 0 \quad \text{on } \Omega, \tag{4.45c}$$

with ∂_ν denoting the outward normal derivative. This formulation, which includes a Robin boundary condition, is aligned with what is typically seen in biomedical optics applications, e.g., [11, 34]. The aforementioned previous works [18, 21, 25, 29] that did not include the isotropic function, ρ_1, in the computation of the interior solution inadvertently computed results for ρ instead of ρ_0. Since the governing equation for ρ is the same as that for ρ_0 and ρ_1, that formal error did not adversely affect the final results in those works.

5. The diffuse reflectance. We have now determined all of the components of the asymptotic solution. We summarize those results here in the context of computing an asymptotic approximation for the diffuse reflectance. Rewriting the diffuse reflectance given in (2.19) in terms of μ and φ, we obtain

$$R_d(x,y,t) = -2\pi \int_{-1}^{0} T^{\text{out}}[\bar{I}](\mu,x,y,0,t)\mu \mathrm{d}\mu \tag{5.1}$$

with

$$\bar{I}(\mu,x,y,z,t) = \frac{1}{2\pi}\int_0^{2\pi} I(\mu,\varphi,x,y,z,t)\mathrm{d}\varphi. \tag{5.2}$$

Substituting (3.2) with the asymptotic expansions we have computed for Φ and Ψ into (5.2), we obtain

$$\bar{I} = \rho_0 + \psi_0^{(0)} + \epsilon(\rho_1 - 3\kappa\mu\partial_z\rho_0 + \psi_1^{(0)}) + O(\epsilon^2). \tag{5.3}$$

The leading order term of the interior solution, ρ_0, satisfies the following initial-boundary value problem for the diffusion equation:

$$\partial_t\rho_0 - \kappa\Delta\rho_0 + \alpha\rho_0 = 0 \quad \text{in } \Omega\times(0,T], \tag{5.4a}$$
$$\rho_0 = cF/a \quad \text{on } \partial\Omega\times(0,T], \tag{5.4b}$$
$$\rho_0|_{t=0} = 0 \quad \text{on } \Omega. \tag{5.4c}$$

The next term of the interior solution, ρ_1, satisfies

$$\partial_t\rho_1 - \kappa\Delta\rho_1 + \alpha\rho_1 = 0 \quad \text{in } \Omega\times(0,T], \tag{5.5a}$$
$$\rho_1 = 3b\kappa\partial_z\rho_0 - \mathbf{d}\cdot\nabla_\perp F \quad \text{on } \partial\Omega\times(0,T], \tag{5.5b}$$
$$\rho_1|_{t=0} = 0 \quad \text{on } \Omega. \tag{5.5c}$$

Upon solution of (5.4), we substitute that result into (4.27) to compute $\psi_0^{(0)}$. We then compute $\psi_1^{(0)}$ through evaluation of (4.29), which depends on $\psi_0^{(1)}$ given by (4.28), $\partial_z\rho_0$, and ρ_1. Substituting these results into (5.3), we obtain

$$\bar{I} = h_1F + h_2(\rho_0+\epsilon\rho_1) + \epsilon 3\kappa h_3\partial_z\rho_0|_{z=0} + \epsilon h_4\partial_x F + \epsilon h_5 \partial_y F + O(\epsilon^2) \quad \text{on } z=0. \tag{5.6}$$

Here,

$$h_1(\mu) = \frac{\mu_0}{2\pi}H^{(0)}(\mu,0^+;\mu_0,0^-), \tag{5.7}$$

$$h_2(\mu) = 1 - \int_0^1 H^{(0)}(\mu,0^+;\mu',0^-)[1-r_F(\mu')]\mu'\mathrm{d}\mu', \tag{5.8}$$

$$h_3(\mu) = -\mu + \int_0^1 H^{(0)}(\mu,0;\mu',0^-)[1+r_F(\mu')]\mu'^2\mathrm{d}\mu', \tag{5.9}$$

$$h_4(\mu) = -\frac{\mu_0}{2\pi}\int_0^\infty\int_0^1 H^{(0)}(\mu,0;\mu',\zeta')\sqrt{1-\mu'^2}\,\mathrm{Re}[H^{(1)}(\mu',\zeta';\mu_0,0)]\mathrm{d}\mu'\mathrm{d}\zeta', \tag{5.10}$$

and

$$h_5(\mu) = \frac{\mu_0}{2\pi}\int_0^\infty\int_0^1 H^{(0)}(\mu,0;\mu',\zeta')\sqrt{1-\mu'^2}\,\mathrm{Im}[H^{(1)}(\mu',\zeta';\mu_0,0)]\mathrm{d}\mu'\mathrm{d}\zeta'. \tag{5.11}$$

Using (5.7)–(5.11), we introduce the quantities

$$R_m = -2\pi \int_{-1}^{0} t_F^{\text{out}}(\mu) h_m(\Upsilon^{-1}(\mu)) \mu \mathrm{d}\mu, \quad m = 1, \dots, 5. \tag{5.12}$$

Then, the diffuse reflectance is given by

$$\begin{aligned} R_d(x,y,t) = {} & R_1 F(x,y,t) + R_2 \rho_0(x,y,0,t) + \epsilon R_2 \rho_1(x,y,0,t) \\ & + \epsilon R_3 3\kappa \partial_z \rho_0(x,y,0,t) + \epsilon R_4 \partial_x F(x,y,t) + \epsilon R_5 \partial_y F(x,y,t) + O(\epsilon^2). \end{aligned} \tag{5.13}$$

Equation (5.13) gives the asymptotic approximation for the diffuse reflectance up to $O(\epsilon^2)$ in terms of ρ_0 satisfying (5.4) and ρ_1 satisfying (5.5), and the incident beam, F. The expansion coefficients, $R_1, \dots, R_5$, can all be readily computed since they correspond to solutions of a one-dimensional half space problem.

The asymptotic model for the steady-state diffuse reflectance, $\tilde{R}_d$, defined in (2.14) is a simplification of (5.13). For this case, F is replaced by $F_0 = t_F^{\text{in}}(\mu_0, \mu_i) f_0(\mu_i x, y)$ from (2.11). In addition, ρ_0 is replaced by the solution of the boundary value problem

$$-\kappa \Delta \tilde{\rho}_0 + \alpha \tilde{\rho}_0 = 0 \quad \text{in } \Omega, \tag{5.14a}$$

$$\tilde{\rho}_0 = c F_0 / a \quad \text{on } \partial\Omega, \tag{5.14b}$$

and ρ_1 is replaced by the solution of the boundary value problem

$$-\kappa \Delta \tilde{\rho}_1 + \alpha \tilde{\rho}_1 = 0 \quad \text{in } \Omega, \tag{5.15a}$$

$$\tilde{\rho}_1 = 3b\kappa \partial_z \tilde{\rho}_0 - \mathbf{d} \cdot \nabla_\perp F_0 \quad \text{on } \partial\Omega. \tag{5.15b}$$

6. Results. In what follows, we show comparisons of the asymptotic approximation for the diffuse reflectance with results computed using the full numerical solution of the radiative transfer equation. First, we consider a specific example to show the characteristic features of the diffuse reflectance. Then we study the error made by the asymptotic approximation for varying values of ϵ to validate the order of the asymptotic approximation. Finally, we study the time-dependent case for the one-dimensional problem to show the multiple time scales contained in the asymptotic model for the diffuse reflectance.

6.1. Spatial distribution of the diffuse reflectance. To demonstrate the effectiveness of the asymptotic approximation in capturing the spatial behavior of the steady-state diffuse reflectance, $\tilde{R}_d$, given in (2.14), we show comparisons with the diffuse reflectance computed from the solution of the full radiative transfer equation for a continuous beam. In particular, we used the Henyey–Greenstein scattering phase function,

$$p(\hat{\mathbf{s}} \cdot \hat{\mathbf{s}}') = \frac{1}{4\pi} \frac{1 - g^2}{(1 + g^2 - 2g \hat{\mathbf{s}} \cdot \hat{\mathbf{s}}')^{3/2}}, \tag{6.1}$$

where $g = \xi_1$ is the anisotropy factor, where ξ_1 is given in (2.4). In the results shown below, we have set $g = 0.8$. In addition, we have set $\epsilon = 0.01$, and $\alpha = 1$. The relative refractive index is set to $n_{\text{rel}} = 1.4$. Rather than prescribe $\tilde{I}_b$, the beam incident on the boundary from outside of the medium, we have set

$$T^{\text{in}}[\tilde{I}_b] = \delta(\mu - \mu_0) \delta(\varphi) \frac{2}{\pi} e^{-2(\mu_0^2 x^2 + y^2)}. \tag{6.2}$$

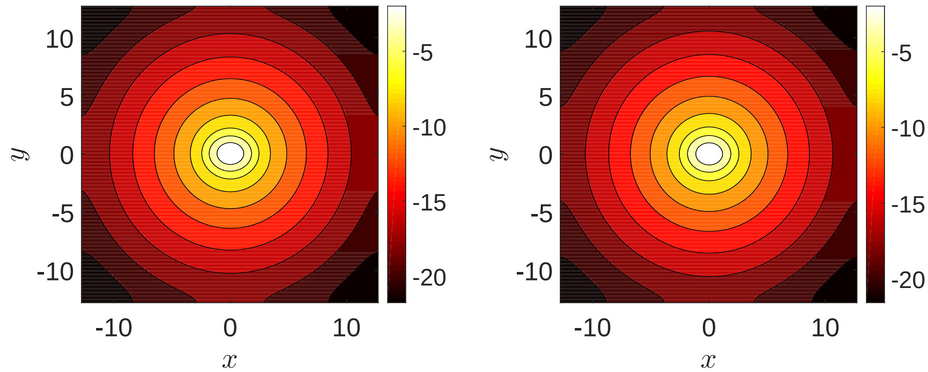

FIG. 1. *A contour plot of* $\log(\tilde{R}_d)$ *as a function of* x *and* y *computed using the numerical solution of the radiative transfer equation (left) and the asymptotic approximation (right) for the incident beam given in* (6.2) *with* $\epsilon = 0.01$ *and* $g = 0.80$.

To solve the radiative transfer equation, we have used the numerical method described in [20]. In the results that follow, we have used a 32-point Gauss–Legendre quadrature rule for μ and a 64-point repeated trapezoid rule for φ. The diffuse reflectance was computed using these quadrature rules over a 256×256 spatial grid for the area, $[-12.8, 12.8] \times [-12.8, 12.8]$, so that the sampling rates are $\Delta x = \Delta y = 0.1$.

To compute the asymptotic approximation for the diffuse reflectance, we have computed the fundamental solution for the half space problem described in section 4.1 using a 32-point Gauss–Legendre quadrature rule. The coefficients, R_m for $m = 1, \ldots, 5$, given in (5.12) are all computed numerically using this same quadrature rule. To compute the solution of boundary value problems (5.14) and (5.15), we Fourier transform the equation and boundary condition in x and y and compute the solution analytically in the transform domain. We compute the inverse Fourier transforms of $\tilde{\rho}_0$ and $\tilde{\rho}_1$ numerically over the same grid used to solve the radiative transfer equation described above.

Since both the numerical solution of the radiative transfer equation and the approximation use the same 32-point Gauss–Legendre quadrature rule, we have chosen μ_0 appearing in (6.2) to coincide with a quadrature point. In particular, for the results shown below, we have set $\mu_0 = 0.7945$ corresponding to $\theta_0 = 37.3935°$.

In Figure 1, we show a contour plot of $\log(\tilde{R}_d)$ as a function of x and y. This result is computed using the numerical solution of the radiative transfer equation (left) and the asymptotic approximation (right). These contour plots show that the diffuse reflectance is peaked about the origin and is not axisymmetric due to the obliquely incident beam. We observe two distinct spatial scales in the diffuse reflectance as the radial distance away from the origin increases. For radial distances approximately less than 4, we find that the diffuse reflectance decays more sharply than for radial distances approximately larger than 4. The faster spatial scale at small radial distances is captured by $\tilde{\rho}_0$ which depends strongly on the features of the incident beam through boundary condition (5.14b). The slower spatial scale at large radial distances is captured by $\tilde{\rho}_1$ and does not depend strongly on the features of the incident beam.

It is clear from Figure 1 that the asymptotic approximation accurately captures the qualitative features of the diffuse reflectance. It does so over several orders of magnitude. In fact, the asymptotic approximation is nearly indistinguishable from the full numerical result. These results show that the asymptotic approximation is a qualitatively accurate model for the diffuse reflectance.

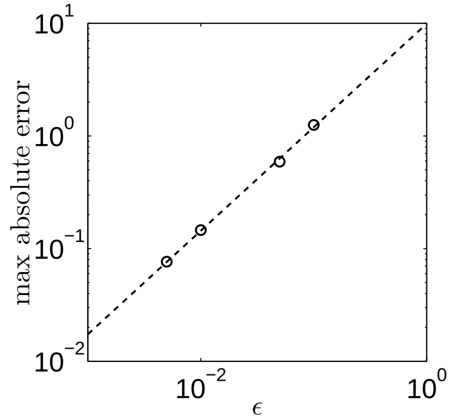

Fig. 2. *Plot of the maximum absolute error made by the asymptotic approximation in comparison with the full numerical solution of the radiative transfer equation as a function of ϵ. The circle symbols give the values computed for $\epsilon = 0.005, 0.01, 0.05$, and 0.1. The dashed curve gives the fitted line through the data. The slope of this line is 2.2932.*

To evaluate the quantitative accuracy of the asymptotic approximation, we computed the absolute error made by the asymptotic approximation for the diffuse reflectance in comparison with the full numerical computation for several different values of ϵ. For this study, we set $g = 0$ so that scattering is isotropic. For both the full numerical solution of the radiative transfer equation and the asymptotic approximation, we have used a 16-point Gauss–Legendre quadrature rule in μ and a 32-point repeated trapezoid rule in φ. We have set the incident beam according to (6.2), but with $\mu_0 = 0.7554$ corresponding to $\theta_0 = 40.9393°$. All other parameters are the same as for the example described above.

Figure 2 shows a log-log plot of the maximum absolute error computed for $\epsilon =$ 0.005, 0.01, 0.05, and 0.1. The circle symbols give the maximum absolute error data. The dashed curve gives the fitted line through these data. The slope of this fitted line is 2.2932, demonstrating the $O(\epsilon^2)$ error associated with the asymptotic approximation. These results show that the asymptotic approximation is a quantitatively accurate model for the diffuse reflectance.

6.2. Time dependence of the diffuse reflectance. To examine the time dependence of the diffuse reflectance, we simplify the problem by considering a pulsed plane wave incident normally on the half space with index-matched boundaries ($n_{\rm rel} = 1$). For that case, the light incident on the half space does not depend on x or y, so $F = F(t)$. Consequently, (5.4) and (5.5) reduce to

$$\partial_t \rho_0 - \kappa \partial_z^2 \rho_0 + \alpha \rho_0 = 0 \quad \text{in } (0,\infty) \times (0,T], \tag{6.3a}$$
$$\rho_0(0,t) = cF(t)/a, \tag{6.3b}$$
$$\rho_0(z,0) = 0 \tag{6.3c}$$

and

$$\partial_t \rho_1 - \kappa \partial_z^2 \rho_1 + \alpha \rho_1 = 0 \quad \text{in } (0,\infty) \times (0,T], \tag{6.4a}$$
$$\rho_1(0,t) = 3b\kappa \partial_z \rho_0(0,t), \tag{6.4b}$$
$$\rho_1(z,0) = 0 \quad \text{on } \Omega, \tag{6.4c}$$

respectively.

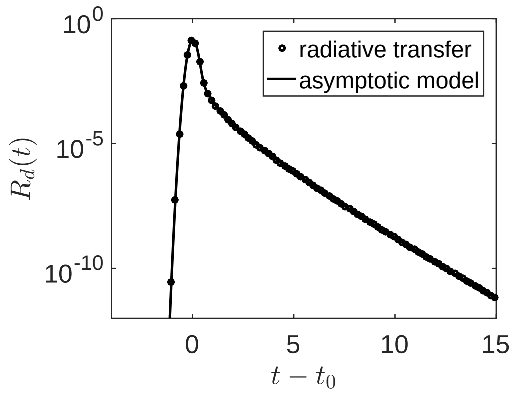

FIG. 3. *Plot of the time-dependent diffuse reflectance due to a pulsed plane wave incident normally on the half space with index-matched boundaries, $\epsilon = 0.01$, and $g = 0.80$. The results computed from the full numerical solution of the radiative transfer equation are plotted as circle symbols, and the asymptotic approximation is plotted as a solid curve. The pulse is $e^{-20(t-t_0)^2}$.*

We use the method given in [19] to solve the time-dependent radiative transfer equation. The asymptotic model for the time-dependent diffuse reflectance depends on F as well as ρ_0, $\partial_z \rho_0$, and ρ_1 evaluated on $z = 0$. Boundary condition (6.3b) gives ρ_0 on $z = 0$, and boundary condition (6.4b) gives ρ_1 on $z = 0$. In fact, because of boundary condition (6.4b), we only need to solve (6.3) and compute $\partial_z \rho_0$ evaluated on $z = 0$. Upon computing that solution, the time-dependent diffuse reflectance is given by

$$R_d(t) = [R_1 + cR_2/a]F(t) + \epsilon 3\kappa [bR_2 + R_3] \partial_z \rho_0|_{z=0}. \tag{6.5}$$

A plot of this time-dependent diffuse reflectance is shown in Figure 3 with $F(t) = e^{-20(t-t_0)^2}$. The results from the radiative transfer equation are plotted as circle symbols and the results from the asymptotic model are plotted as a solid curve. The asymptotic model is indistinguishable from the radiative transfer equation results. We find that the maximum absolute error made by the asymptotic model is 0.0015.

This result shows the multiple time scales in the diffuse reflectance. The short time behavior corresponds to the immediate reflection of the incident pulse by the scattering medium and is modeled by the terms in (6.5) proportional to $F(t)$. The long time behavior corresponds to the terms in (6.5) proportional to $\partial_z \rho_0$. These terms model light that has penetrated deep into the half space before emerging as backscattered light. In fact, this short and long time behavior is what motivated Brauns [1] to use a biexponential model to fit the ultrafast measurements.

7. Conclusions. We have computed an asymptotic model for the diffuse reflectance due to continuous and pulsed beams obliquely incident on a half space composed of a strongly scattering and weakly absorbing medium. This problem was motivated by recent technological advances made in ultrafast measurements of the time-dependent diffuse reflectance at midinfrared wavelengths [1]. Because these ultrafast measurements provide access to studying effective path lengths of photons traveling in a scattering medium, it is crucial for this problem to develop predictive models that accurately capture the multiscale behavior in space and time.

This asymptotic model is much simpler to compute than the solution of the boundary (continuous beam) value and initial-boundary (pulsed beam) problems for the radiative transfer equation that govern this problem. Instead, this asymptotic model requires the solution of initial-boundary or boundary value problems for the diffusion equation and a one-dimensional radiative transfer equation for the boundary layer solution. The diffusion equation can be solved using standard methods. Using numerical calculations, we are able to explicitly solve the one-dimensional radiative transfer equation.

With regard to midinfrared diffuse reflectance spectroscopy, this asymptotic model provides valuable insight into information contained in measurements. In particular, this asymptotic model provides insight on how to partition the measured data in a meaningful way. Suppose that the scattering phase function is known. For that case, all of the coefficients in the asymptotic diffuse reflectance model given in (5.13) can be computed explicitly. The $O(1)$ terms in (5.13) are so-called instrument response terms since they are proportional to the incident pulse. Moreover, if that pulse is short, the $O(1)$ contribution to the diffuse reflectance is also short. The long time behavior is modeled accurately by the diffusion equation in which the absorption coefficient appears as a linear loss term. Recovering this absorption coefficient from these measurements then becomes a relatively straightforward parameter estimation problem. Although diffusion approximations appearing in the applied literature seek only to model the long time behavior of the diffuse reflectance, their use of phenomenological boundary conditions and source terms leads to $O(1)$ errors. These errors affect the overall ability to estimate the parameters sought. Ultrafast measurements of the diffuse reflectance made these errors even more apparent, rendering these diffusion approximations ineffective. The final results for the asymptotic model for the diffuse reflectance have been shown to accurately capture the multiscale behavior of the diffuse reflectance in space and time. These results suggest that this asymptotic model should be extremely useful for problems in midinfrared diffuse reflectance spectroscopy.

Acknowledgments. The authors are grateful to Dr. Peter Griffiths and Dr. Eric Brauns for their helpful discussions on diffuse reflectance spectroscopy.

REFERENCES

[1] E. B. Brauns, *Midinfrared diffuse reflection on ultrafast time scales*, Appl. Spectrosc., 68 (2014), pp. 1–4.
[2] S. Chandrasekhar, *Radiative Transfer*, Dover, New York, 1960.
[3] D. J. Dahm and K. D. Dahm, *Interpreting Diffuse Reflectance and Transmittance*, NIR, Chichester, UK, 2007.
[4] S. Fantini, M. A. Franceschini, and E. Gratton, *Effective source term in the diffusion equation for photon transport in turbid media*, Appl. Opt., 36 (1997), pp. 156–163.
[5] T. J. Farrell, M. S. Patterson, and B. Wilson, *A diffusion theory model of spatially resolved, steady-state diffuse reflectance for the noninvasive determination of tissue optical properties invivo*, Med. Phys., 19 (1992), pp. 879–888.
[6] P. R. Griffiths and J. A. de Haseth, *Fourier Transform Infrared Spectrometry*, Wiley, New York, 2007.
[7] G. Habetler and B. Matkowsky, *Uniform asymptotic expansions in transport theory with small mean free paths, and the diffusion approximation*, J. Math. Phys., 16 (1975), pp. 846–854.
[8] R. C. Haskell, L. O. Svaasand, T.-T. Tsay, T.-C. Feng, B. J. Tromberg, and M. S. McAdams, *Boundary conditions for the diffusion equation in radiative transfer*, J. Opt. Soc. Am. A, 11 (1994), pp. 2727–2741.

[9] A. H. Hielscher, S. L. Jacques, L. Wang, and F. Tittel, *The influence of boundary conditions on the accuracy of diffusion theory in time-resolved reflectance spectroscopy of biological tissues*, Phys. Med. Biol., 40 (1995), p. 1957.

[10] X. Intes, B. L. Jeune, F. Pellen, Y. Guern, J. Cariou, and J. Lotrian, *Localization of the virtual point source used in the diffusion approximation to model a collimated beam source*, Wave Random Media, 9 (1999), pp. 489–499.

[11] A. Ishimaru, *Wave Propagation and Scattering in Random Media*, Wiley, New York, 1997.

[12] A. Ishimaru, Y. Kuga, R. L.-T. Cheung, and K. Shimizu, *Scattering and diffusion of a beam wave in randomly distributed scatterers*, J. Opt. Soc. Am., 73 (1983), pp. 131–136.

[13] S. L. Jacques, *Light distributions from point, line and plane sources for photochemical reactions and fluorescence in turbid biological tissues*, Photochem. Photobiol., 67 (1998), pp. 23–32.

[14] H. W. Jensen, *Realistic Image Synthesis Using Photon Mapping*, AK Peters, Natick, MA, 2001.

[15] M. Jia, X. Chen, H. Zhao, S. Cui, M. Liu, L. Liu, and F. Gao, *Virtual-source diffusion approximation for enhanced near-field modeling of photon-migration in low-albedo medium*, Opt. Express, 23 (2015), pp. 1337–1352.

[16] A. Kienle and M. S. Patterson, *Improved solutions of the steady-state and the time-resolved diffusion equations for reflectance from a semi-infinite turbid medium*, J. Opt. Soc. Am. A, 14 (1997), pp. 246–254.

[17] A. D. Kim, *Transport theory for light propagation in biological tissue*, J. Opt. Soc. Am. A, 21 (2004), pp. 820–827.

[18] A. D. Kim, *Correcting the diffusion approximation at the boundary*, J. Opt. Soc. Am. A, 28 (2011), pp. 1007–1015.

[19] A. D. Kim and A. Ishimaru, *Optical diffusion of continuous-wave, pulsed, and density waves in scattering media and comparisons with radiative transfer*, Appl. Opt., 37 (1998), pp. 5313–5319.

[20] A. D. Kim and M. Moscoso, *Beam propagation in sharply peaked forward scattering media*, J. Opt. Soc. Am. A, 21 (2004), pp. 797–803.

[21] A. D. Kim and M. Moscoso, *Diffusion of polarized light*, Multiscale Model. Simul., 9 (2011), pp. 1624–1645.

[22] G. Kortüm, *Reflectance Spectroscopy: Principles, Methods, Applications*, Springer, New York, 2012.

[23] A. F. Kostko and V. A. Pavlov, *Location of the effective diffusing-photon source in a strongly scattering medium*, Appl. Opt., 36 (1997), pp. 7577–7582.

[24] E. W. Larsen and J. B. Keller, *Asymptotic solution of neutron transport problems for small mean free paths*, J. Math. Phys., 15 (1974), pp. 75–81.

[25] O. Lehtikangas, T. Tarvainen, and A. D. Kim, *Modeling boundary measurements of scattered light using the corrected diffusion approximation*, Biomed. Opt. Express, 3 (2012), pp. 552–571.

[26] F. Malvagi and G. Pomraning, *Initial and boundary conditions for diffusive linear transport problems*, J. Math. Phys., 32 (1991), pp. 805–820.

[27] M. S. Patterson, B. Chance, and B. C. Wilson, *Time resolved reflectance and transmittance for the noninvasive measurement of tissue optical properties*, Appl. Opt., 28 (1989), pp. 2331–2336.

[28] G. Pomraning and B. Ganapol, *Asymptotically consistent reflection boundary conditions for diffusion theory*, Ann. Nucl. Energy, 22 (1995), pp. 787–817.

[29] S. B. Rohde and A. D. Kim, *Modeling the diffuse reflectance due to a narrow beam incident on a turbid medium*, J. Opt. Soc. Am. A, 29 (2012), pp. 231–238.

[30] T. Spott and L. O. Svaasand, *Collimated light sources in the diffusion approximation*, Appl. Opt., 39 (2000), pp. 6453–6465.

[31] G. E. Thomas and K. Stamnes, *Radiative Transfer in the Atmosphere and Ocean*, Cambridge University Press, Cambridge, UK, 2002.

[32] L. Wang and S. L. Jacques, *Use of a laser beam with an oblique angle of incidence to measure the reduced scattering coefficient of a turbid medium*, Appl. Opt., 34 (1995), pp. 2362–2366.

[33] L. V. Wang and S. L. Jacques, *Source of error in calculation of optical diffuse reflectance from turbid media using diffusion theory*, Comput. Meth. Prog. Bio., 61 (2000), pp. 163–170.

[34] L. V. Wang and H.-I. Wu, *Biomedical Optics: Principles and Imaging*, Wiley, New York, 2012.